

# **Maximizing utilization of carbon fibers by bimetallic-catalytic etching and electrochemical modification for difunctional aqueous supercapacitors**

*Jie Zhang<sup>1,2</sup>, Hao Zhang<sup>1,2</sup>, Wenli Li<sup>1,2</sup>, Guangwen Xu<sup>1</sup>, Yanbin Cui<sup>1,2,\*</sup>*

<sup>1</sup>State Key Laboratory of Multiphase Complex Systems, Institute of Process Engineering, Chinese Academy of Sciences, Beijing 100190, China

<sup>2</sup> Center of Materials Science and Optoelectronics Engineering, University of Chinese Academy of Sciences, Beijing 100049, China

\*E-mail: [ybcui@ipe.ac.cn](mailto:ybcui@ipe.ac.cn)

\*Corresponding author: Prof. Yanbin Cui

# **Supporting information**

## **Experimental Section**

### **Preparation of Lg-CC**

The Co-Fe LDH nanosheets were synthesized by a cathodic electrodeposition method in a standard three-electrode cell in which a piece of carbon cloth ( $2 \times 1 \text{ cm}^2$ , 0.33 mm in thickness), Pt foil, and Saturated calomel electrode (SCE) were used as the working electrode, the counter electrode, and the reference electrode, respectively. Specifically, a precursor solution of  $\text{Co}(\text{NO}_3)_2 \cdot 6\text{H}_2\text{O}$  (15 mmol) and  $\text{Fe}(\text{NO}_3)_3 \cdot 9\text{H}_2\text{O}$  (5 mmol) was performed at a constant potential of -1.3 V for 80 s (Temperature:  $\sim 25^\circ\text{C}$ ). The obtained Co-Fe LDH/CC catalyst was then annealed at  $900^\circ\text{C}$  for 80 min under the  $\text{CO}_2$  atmosphere, followed by immersing in 3 M HCl overnight. Finally, the product was washed several times with DI water to remove the residual acid and dried at  $60^\circ\text{C}$ . Afterwards, the O-CC sample was prepared as the similar process with that of Lg-CC except for the loading Co-Fe LDH.

### **Preparation of Ralg-CC**

The Lg-CC as a working electrode was activated electrochemically for 2 h at a constant potential of 2.2 V in 1 M  $\text{Na}_2\text{SO}_4$  aqueous solution followed by electrochemical reduction in same system at 50 mV/s in the potential window of -1.5~0.8 V and conducted for 50 cycles to obtain Ralg-CC.

### **Fabrication of flexible asymmetric supercapacitor**

To balance the charge of negative electrode, onion-like MnO<sub>2</sub>/CC (O-MnO<sub>2</sub>/CC) positive electrode was fabricated using a step-wise electroplating method in a Mn(CH<sub>3</sub>COO)<sub>2</sub>·4H<sub>2</sub>O (0.4 M) and Na<sub>2</sub>SO<sub>4</sub> (0.6 M) solution at two different operation voltages 3 V (250 s) and 1 V (100 s) among three-electrode system containing Lg-CC as working electrode, a Pt foil as counter electrode, and a saturated calomel electrode (SCE) as reference electrode. The mass loading of the positive electrodes was controlled based on the charge balance equation ( $C_+V_+=C_-V_-$ ). Besides, after immersing a piece of cellulose paper (NKK-MPF30AC-100, Japan) in a 1 M Na<sub>2</sub>SO<sub>4</sub> aqueous solution for 10 min, a separator was obtained and then carefully entangled with the O-MnO<sub>2</sub>/ACC and Ralg/CC. Eventually, the assembled device was wrapped with a thin parafilm to prevent the volatilization of water.

## **Materials characterization**

The X-ray diffraction (XRD) patterns were collected by a Rigaku Smartlab X-ray diffractometer using Cu K $\alpha$  radiation. The morphology and microstructure images were observed by a JEM-7001F scanning electronic microscope (SEM) and a JEOL-2100 transmission electron microscope (TEM). Raman spectra were recorded by a confocal laser inVia Raman microscope (Renishaw,  $\lambda_e = 514\text{nm}$ ). The pore size distribution curve was produced from the isotherm by Density Functional Theory (NLDFT) methods. X-ray photoelectron spectroscopy (XPS) measurements of the samples were fulfilled by utilizing a Thermal-Fisher ESCALAB 250Xi X-ray spectrophotometer. The water contact angle was measured by the optical contact angle measurement system (DSA100S, KRUSS GmbH, Germany). Cyclic

voltammetry (CV), galvanostatic charge/discharge (GCD), as well as electrochemical impedance spectroscopy (EIS) of the individual electrode were carried out in a three-electrode electrochemical work station having Platinum and Saturated calomel electrode as counter and reference electrode, respectively. The aqueous electrolyte for Zn ion supercapacitor was 1M ZnSO<sub>4</sub>/1 M Na<sub>2</sub>SO<sub>4</sub>.

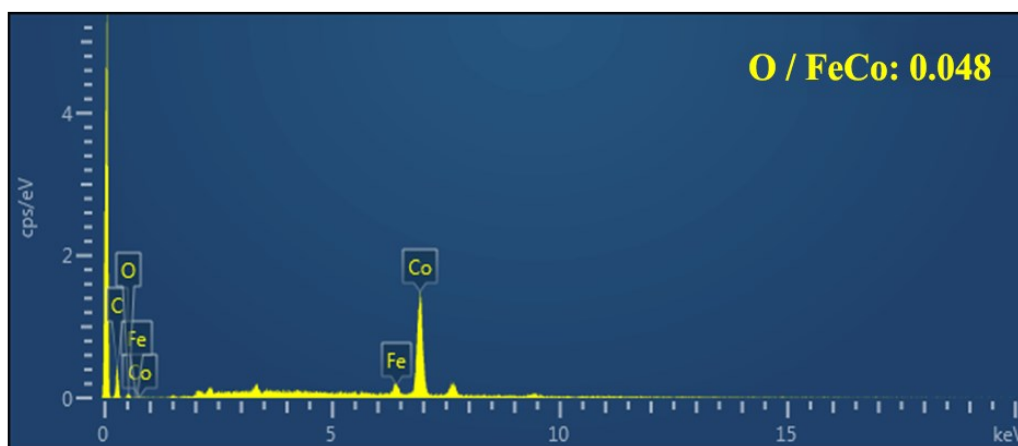


Fig. S1 EDS image of carbon cloth loaded with LDH precursors thermally treated at at 800 °C.

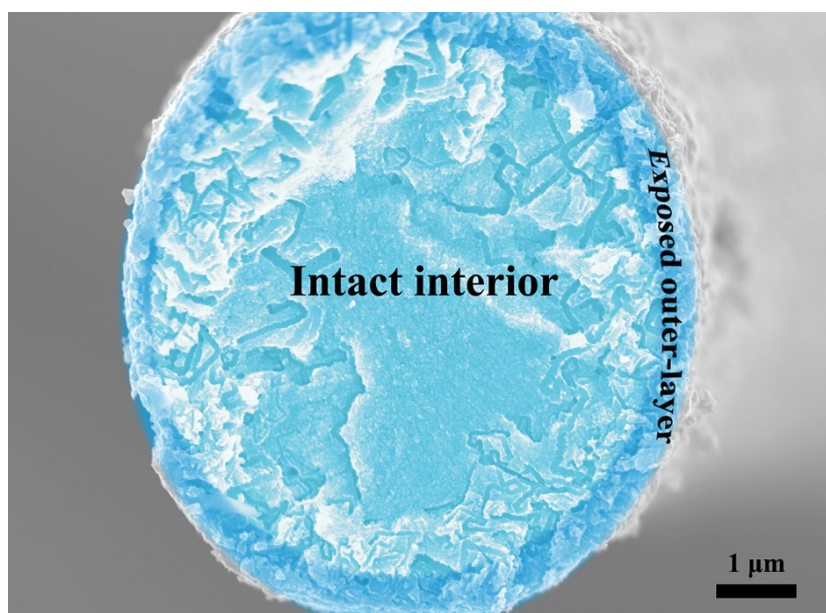


Fig. S2 Cross-sectional SEM image of Ralg-CC.

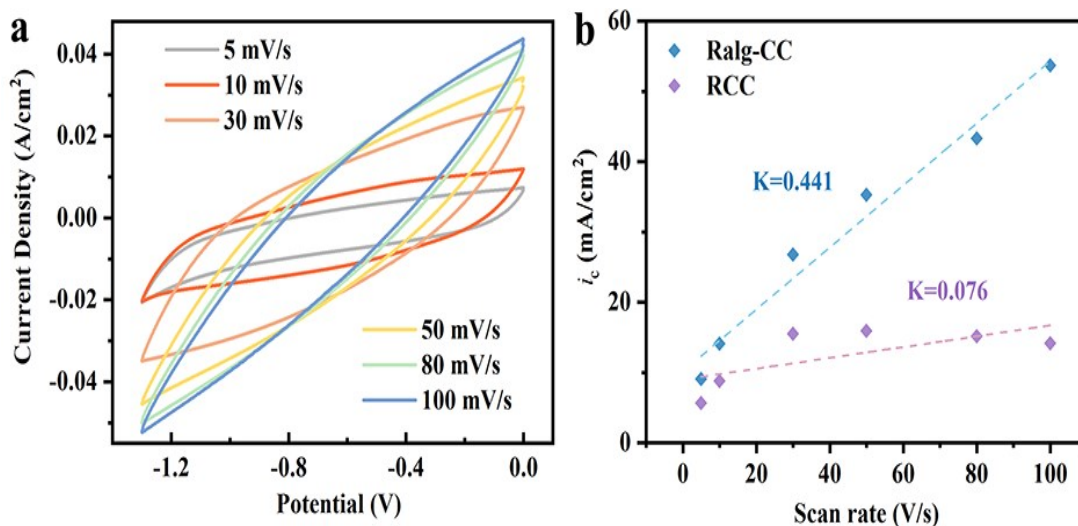


Fig. S3 (a) CV curves of RCC at various scan rates. (b) The halves of the anodic and cathodic current measured at -0.6 V vs SCE plotted as a function of scan rate.

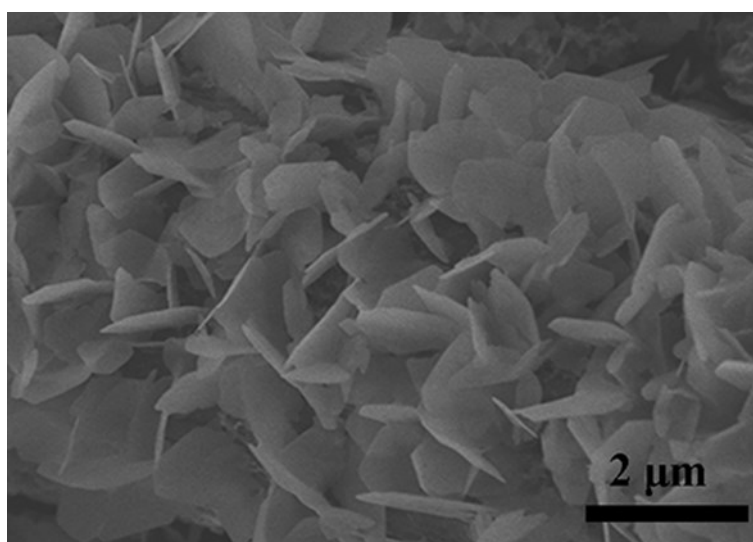


Fig. S4 SEM image of Ralg-CC after the cycling test in  $\text{ZnSO}_4/\text{Na}_2\text{SO}_4$  electrolyte.

**Table S1** Comparison study on the electrochemical performance of Ralg-CC in this work with previously reported results.

Active materials	Electrolyte	Potential (V)	Capacitance (mF/cm <sup>2</sup> )	Ref.
Activated Carbon Felt	1M Na <sub>2</sub> SO <sub>4</sub>	-1~0	907.83	[1]

<b>MOF-derived N-doped carbon bubbles/carbon tube arrays</b>	1M H <sub>2</sub> SO <sub>4</sub>	0~1	~370	[2]
<b>CC@CoO@S-Co<sub>3</sub>O<sub>4</sub></b>	2M KOH	0~0.45	873	[3]
<b>PANI/ZnO/ZIF-8/Graphene/ polyester</b>	3M KCl	-0.2~1	~750	[4]
<b>Co-Mn MOF</b>	2M KOH	0~0.35	~600	[5]
<b>CoP/Carbon Cloth</b>	1M LiCl	-0.8~0	571.3	[6]
<b>Electrochemically pretreated carbon nanotube film/PPY</b>	5M LiCl	-1~0.1	965.3	[7]
<b>MoS<sub>2</sub>@CTNT</b>	0.5M Na <sub>2</sub> SO <sub>4</sub>	-0.8~0	557.83	[8]
<b>H-VO<sub>x</sub>/CC</b>	5M LiCl	-1~0	554	[9]
<b>Ralg-CC</b>	<b>1M Na<sub>2</sub>SO<sub>4</sub></b>	<b>-1.3~0</b>	<b>1089</b>	<b>This work</b>

## References:

1. G. Lou, Y. Wu, X. Zhu, Y. Lu, S. Yu, C. Yang, H. Chen, C. Guan, L. Li and Z. Shen, *ACS applied materials & interfaces*, 2018, 10, 42503-42512.
2. Z. Tang, G. Zhang, H. Zhang, L. Wang, H. Shi, D. Wei and H. Duan, *Energy Storage Materials*, 2018, 10, 75-84.
3. S. Dai, Y. Yuan, J. Yu, J. Tang, J. Zhou and W. Tang, *Nanoscale*, 2018, 10, 15454-15461.
4. Y.-N. Liu, L.-N. Jin, H.-T. Wang, X.-H. Kang and S.-W. Bian, *J Colloid Interf Sci*, 2018, 530, 29-36.
5. S. H. Kazemi, B. Hosseinzadeh, H. Kazemi, M. A. Kiani and S. Hajati, *ACS Applied Materials & Interfaces*, 2018, 10, 23063-23073.
6. Z. Zheng, M. Retana, X. Hu, R. Luna, Y. H. Ikuhara and W. Zhou, *ACS*

*Applied Materials & Interfaces*, 2017, 9, 16986-16994.

7. Z.-H. Chang, D.-Y. Feng, Z.-H. Huang and X.-X. Liu, *Chem Eng J*, 2018, 337, 552-559.
8. W Cao, Y Gong, W Wang, M Chen, J Yang, Y Xue, *Nanoscale*, 2021, 13, 8658-8664.
9. S Chen, H Jiang, Q Cheng, G Wang, S Petr, C Li, *Chem Eng J*, 2021, 403, 126380.